A&A 397, 213–226 (2003)
DOI: 10.1051/0004-6361:20021466

Astronomy & Astrophysics

A radio catalog of Galactic HII regions for applications from decimeter to millimeter wavelengths⋆

R. Paladini[1], C. Burigana[2], R. D. Davies[3], D. Maino[4,5], M. Bersanelli[5,6], B. Cappellini[5], P. Platania[5], and G. Smoot[7]

[1] SISSA, International School for Advanced Studies, via Beirut 2-4, 34014 Trieste, Italy
[2] IASF, Istituto di Astrofisica Spaziale e Fisica Cosmica, Sezione di Bologna – Consiglio Nazionale delle Ricerche, via Gobetti 101, 40129 Bologna, Italy
[3] University of Manchester, Jodrell Bank Observatory, Macclesfield – Cheshire SK11 9DL, UK
[4] Osservatorio Astronomico di Trieste, via G. B. Tiepolo 11, 34131 Trieste, Italy
[5] Università degli Studi di Milano, via Celoria 16, 20133 Milano, Italy
[6] IASF, Istituto di Astrofisica Spaziale e Fisica Cosmica, Sezione di Milano – Consiglio Nazionale delle Ricerche, via Bassini 15, 20133 Milano, Italy
[7] LBNL, SSL, Physics Department, University of California, Berkeley, CA 94720, USA

Received 26 July 2002 / Accepted 1 October 2002

Abstract. By collecting the information from 24 previously published lists and catalogs, we produce a comprehensive catalog (Master Catalog) of 1442 Galactic HII regions. For each object, we quote the original fluxes and diameters as well as the available information on radio line velocities, line widths and line temperatures and the errors on these quantitities. References to the original works are also reported. By exploiting all these data we produce a Synthetic Catalog of fluxes and diameters (with corresponding errors) at 2.7 GHz. This choice is motivated by the extensive, although not complete, information available at this frequency, widely spread among many different catalogs, and by its relevance for both detailed studies on Galactic HII regions and the extrapolation up to millimetric wavelengths. The catalog can be used for detailed studies of Galactic HII regions and, by extrapolation, for investigations of HII regions up to millimetric wavelengths. In particular, we discuss the study of the effects of microwave emission from HII regions on the new generation of Cosmic Microwave Background (CMB) experiments. We present simulations of the detection of HII regions in the Planck high resolution CMB survey, and briefly analize some of the typical applications of our catalog to the evaluation of CMB anisotropy experiments such as calibration, beam reconstruction and straylight effects. The Master Catalog and the Synthetic Catalog are available via ftp at: `cdsarc.u-strasbg.fr`. This work is related to Planck-LFI activities.

Key words. HII regions – catalogs – cosmic microwave background

1. Introduction

HII regions are very important radio sources within our Galaxy. They not only provide information about the early stages of stellar formation but represent also a unique tool to investigate the Galactic spiral structure. Moreover, their radio emission, not attenuated by dust extinction, is powerful enough to enable us to probe distant parts of the Galactic plane. Despite their astrophysical relevance, there is no currently available comprehensive catalog of these objects. A few optical catalogs (Sharpless 1959; Marsálková 1974; Fich & Blitz 1982) do exist but they are severely limited by the dust obscuration effects mentioned above. At radio wavelengths, the most comprehensive catalog of diffuse brightness nebulae is the *COBE*-HII Catalog at 2.7 GHz (Witebsky 1978a,b). It includes 909 objects and has provided a reliable tool for estimating the contribution of HII regions to Galactic free-free in the analysis of the *COBE* data. More recently, a list of 760 objects with angular diameter less than 10′ has been compiled by Kuchar & Clark 1997 from the Green Bank (Condon et al. 1989) and Parkes-MIT-NRAO (Condon et al. 1993; Tasker et al. 1994) radio surveys at 4.85 GHz.

These catalogs can now be combined and updated with other recently published data. A strong motivation supporting this work is its relevance to cosmic microwave background (CMB) studies. Since the successful results of the *COBE* satellite (Smoot et al. 1992), increasing efforts have been devoted to investigating the cosmological information contained in the CMB anisotropies. Recent balloon experiments such as BOOMERANG (de Bernardis et al. 2000) and MAXIMA-1 (Hanany et al. 2000) as well as ground interferometer experiments as DASI (Leitch et al. 2002), CBI (Mason et al. 2001) and VSA (Scott et al. 2002) have achieved remarkable results

Send offprint requests to: R. Paladini, e-mail: `paladini@sissa.it`

⋆ The Master Catalog and the Synthetic Catalog are only available in electronic form via anonymous ftp to
`cdsarc.u-strasbg.fr (130.79.128.5)`
or via
`http://cdsweb.u-strasbg.fr/cgi-bin/qcat?J/A+A/397/213`

but, at the same time, have shown the necessity to improve our knowledge of all the relevant astrophysical foregrounds which may affect the recovery of the CMB angular power spectrum and, ultimately, of the cosmological parameters. In particular, the free-free emission is the least known among the Galactic foregrounds. However, much of the free-free emission at low Galactic latitudes is produced by individual bright HII regions. Because of their strong emission, they may represent a potential source of contamination for the new generation of nearly full-sky coverage CMB anisotropy space missions at high sensitivity and resolution. These sources are also good candidates for receiver and antenna pattern calibration.

By collecting the information from 24 previously published lists and catalogs, we present in this paper a comprehensive catalog (Master Catalog) of 1442 Galactic HII regions. For each object, we quote the original fluxes and diameters as well as the available information on radio recombination line velocities, line widths and line temperatures and the errors on all these quantitities.

By exploiting these data we produce a Synthetic Catalog of fluxes and diameters (with corresponding errors) at 2.7 GHz, motivated by the extensive although not complete information available at this frequency, widely spread among the different catalogs, and by its relevance for both detailed studies on Galactic HII regions and the extrapolation up to millimetric wavelengths. We discuss also some possible applications of this Synthetic Catalog to CMB studies. The paper is organized as follows. Section 2 presents the stages of the Master Catalog compilation (e.g., the selection criteria for the reference papers and the removal of non-thermal sources) and briefly summarizes the content of the final compilation, while an accurate and full description of the catalog content is given in Appendix I. Section 3 describes the production of the Synthetic Catalog at 2.7 GHz. Section 4 concerns the completeness and flux limit of the catalog and the spatial distribution of the listed sources. Perspectives of possible applications of this Synthetic Catalog to CMB studies are presented in Sect. 5. Finally, we draw our main conclusions in Sect. 6.

2. The Master Catalog compilation

In this section we discuss the data processing which was applied to convert the information from the various reference catalogs into a uniform format for easy intercomparison in a Master Catalog.

2.1. Selection of the original catalogs

The Master Catalog was compiled from the 24 radio catalogs shown in Table 1. We follow the classification of HII regions by Lockman et al. (1996) and only include catalogs of diffuse and compact HII regions. Surveys of ultra-compact (UCHII) and extremely extended objects (EHE) will be considered in a forthcoming extension of the present list: they are bright in the infrared (UCHII) and in the optical (EHE) but relatively weak at radio frequencies.

The reason for following this route is driven by the general goals of the work. Planned and on-going CMB experiments typically have angular resolutions ranging from a few arcmin up to tens of arcmin in order to exploit the wealth of cosmological information encoded in the CMB anisotropies. Therefore, diffuse and compact HII regions – with a typical angular extension of a few arcmin – are the most important to be taken into account if we want to investigate the free-free emission as a contaminant of the CMB.

We have therefore considered single-dish medium-resolution observations, typically with beamwidths of a few arcmin, rather than interferometer or synthesis telescope surveys (Becker et al. 1994; Taylor et al. 1996) which usually achieve a resolution of a few arcsec. Also, single-dish low-resolution observations (Westerhout 1958; Wilson & Bolton 1960), whose typical angular resolution is $\sim 1^\circ$, have not been included in the sample of selected references in order to avoid problems arising from double-counting of the sources. Likewise we have not considered surveys simply oriented to the study of the morphology and spectral behaviour of the diffuse Galactic radiation at centimetric wavelengths (Reich et al. 1984; Reich et al. 1990; Fürst et al. 1990a; Fürst et al. 1990b; Duncan et al. 1995).

2.2. Identification and removal of SNRs

The selected catalogs may contain in principle also some Galactic sources, different from HII regions, that we need to exclude from our Master Catalog compilation. Therefore, supernova remnants (SNRs) of each selected catalog have been identified by comparing the coordinates of the catalog sources with those of the catalog of Galactic supernova remnants by Green (2000). The identification has been performed taking into account the average position uncertainty of the selected catalogs of HII regions and of the Green Catalog (both $\sim 1'$).

2.3. Quoted flux densities and angular diameters

We provide the flux densities integrated over each source, S, and the source angular diameter, $\Theta_{\rm HII}$. In a few references (Wink et al. 1982 at 86 GHz; Wink et al. 1983) the flux density is given only as a peak value. We correct this to a true value by assuming that the source has a Gaussian profile and using the observed diameter (see Rohlfs 1990).

The source angular diameter is given in terms of observed diameter in a few references (Altenhoff et al. 1979; Downes et al. 1980; Wink et al. 1983). We derive a true diameter again assuming a Gaussian source profile. For source dimensions significantly smaller than the beamwidth, the references give upper limit diameters. The Master Catalogs includes these derived flux densities and diameters for completeness.

2.4. Other relevant data

In addition to the basic data on flux density and diameter, for each source there are available further relevant data which make the catalog more useful.

We include the notes from Kuchar & Clark (1997) on the environment of each source, indicating whether the source is complex or if it has a strong source nearby. Again, following

Table 1. List of the references (in alphabetical order) for the catalog. Listed $l_{\rm min}$ and $l_{\rm max}$ provide the longitude range spanned by each survey. The range in latitude is $|b| \leq 2^\circ - 4^\circ$.
† Number of sources after subtraction of nonthermal objects. Notes: (*a*) the list of sources is retrieved by the intersection with the radio recombination line survey by Lockman et al. (1989); (*b*) early Parkes survey at 2.7 GHz; (*c*) Effelberg 100-m survey at 2.7 GHz; (*d*) Cygnus X; (*e*) nonuniform sky coverage; (*f*) Green Bank and Parkes-MIT-NRAO surveys cover almost the whole sky: HII regions have been identified from either optical or radio recombination line surveys along the disk.

Reference	$l_{\rm min}$	$l_{\rm max}$	ν (GHz)	HPBW (′)	Number† of sources
Altenhoff et al. (1970)	335°	75°	1.4/2.7/5	10	325
Altenhoff et al. (1979)[a]	2°	60°	5	2.6	265
Beard (1966)[b]	331°	333°	2.7	7.4	13
Beard & Kerr (1969)[b]	27°	38°	2.7	7.4	34
Beard et al. (1969)[b]	345°	5°	2.7	7.4	72
Berlin et al. (1985)	4°	10°	3.9	0.8×18.3	45
Caswell & Haynes (1987)	190°	40°	5	4.2	308
Day et al. (1969)[b]	307°	330°	2.7	8.2	109
Day et al. (1970)[b]	37°	47°	2.7	8.2	48
Downes et al. (1980)	357°	60°	5	2.6	169
Felli & Churchwell (1972)	(*e*)	(*e*)	1.4	10	80
Fürst et al. (1987)[c]	(*e*)	(*e*)	2.7	4.27	7
Goss & Day (1970)[b]	6°	26°	2.7	8	85
Kuchar & Clark (1997)	(*f*)	(*f*)	4.8	3.1/4.2	760
Mezger & Henderson (1967)	(*e*)	(*f*)	5	6.3	17
Reich et al. (1986)[c]	(*e*)	(*e*)	2.7	4.27	5
Reifenstein et al. (1970)	348°	80°	5	6.5	105
Thomas & Day (1969a)[b]	288°	307°	2.7	8.2	39
Thomas & Day (1969b)[b]	334°	345°	2.7	8.2	29
Wendker (1970)[d]	76°	84°	2.7	11	77
Wilson et al. (1970)	282°	346°	5	4	132
Wink et al. (1982)	(*e*)	(*e*)	5/15/86	2.6/1/1.3	112
Wink et al. (1983)	359°	50°	14.7	1	84

Kuchar & Clark (1997) we give radio counterparts in other catalogs other than those referred to in Sect. 2.1. Optical counterparts of the unobscured sources are obtained from the identification given in the Catalog by Márs alková (1974).

We include available radio recombination line data because they provide important information on kinematics, distances and electron density for each HII region. The data are given by Downes et al. (1980), Caswell & Haynes (1987), Kuchar & Clark (1997), Reifenstein et al. (1970), Wilson et al. (1970), Wink et al. (1982) and Wink et al. (1983) in the source catalogs listed in Sect. 2.1 and are complemented by the recombination line data of Lockman (1989).

2.5. The Master Catalog

All sources observed at least by one of the surveys of Table 1 and recognized as Galactic HII regions were included in the Master Catalog. 1442 sources are listed. All relevant information from each of the reference catalogs is retained. Data for individual HII regions are available from the references at 8 frequencies (1.4, 2.7, 3.9, 4.8, 5., 14.7, 15 and 86 GHz). This large data base is presented in a readily accessible form as 11 *sub-catalogs*:

sub-catalog 1 coordinates (epoch 2000) and remarks
sub-catalog 2 / 3 flux density (Jy) / 1–σ (%) error
sub-catalog 4 / 5 diameter (arcmin) / 1–σ (%) error
sub-catalog 6 / 7 line velocity (km s^{-1}) / 1–σ error (km s^{-1})
sub-catalog 8 / 9 line width (km s^{-1}) / 1–σ error (km s^{-1})
sub-catalog 10 / 11 line temperature (K) / 1–σ error (K).

The sub-catalogs give, for each source, an identification number along with the position in Galactic and celestial coordinates. Apart from sub-catalog 1, each sub-catalog has 37 columns. The columns are in order of increasing frequency of observation; at each frequency the columns are in alphabetical order of the references in Table 1. We note that for sub-catalog 6–11 (the radio recombination line data) the observations may refer to frequencies other than those in the main continuum catalog (in this case, the line frequency is reported).

Appendix I gives a detailed description of the content of each sub-catalog.

3. The Synthetic Catalog at 2.7 GHz

The final task in bringing together the wide-spread radio data on HII regions is to construct a readily accessible catalog summarizing the basic information on each of the 1442 sources covered in the comprehensive data base of the Master Catalog. This Synthetic Catalog gives the best available data on flux density, angular diameter and, where available, the line velocity.

2.7 GHz was chosen as the base frequency for the Synthetic Catalog; it lies in the middle of the frequency range of those catalogs containing most of the data, namely 1.4, 2.7

and 5 GHz. Since there is not complete source coverage at any one frequency, we derive the flux density at 2.7 GHz from the observed frequencies for all the sources. We now describe how best-estimate values of the flux density, diameter and velocity with corresponding error estimates are derived from the Master Catalog.

3.1. Flux density estimates at 2.7 GHz

We estimate the flux density at 2.7 GHz in four different ways:

1. we use the flux density measures at 2.7 GHz when these are available;
2. if there are no flux density measures at 2.7 GHz and there are available measures at only one other frequency, we extrapolate these values to 2.7 GHz with the theoretical spectral index $\alpha = -0.1$ ($S \propto \nu^{\alpha}$) which is typical of thermal bremsstrahlung emission in a thin plasma;
3. if there are flux density measures only at frequencies $\geq$14.7 GHz, we first select the lowest among the given frequencies – averaging over 14.7 and 15 GHz when both are available – and then extrapolate to 2.7 GHz with $\alpha = -0.1$;
4. if there are only flux density measures at frequencies other than 2.7 GHz and at least one measure at $\nu \leq 5$ GHz, we follow these lines: we exclude the values at 3.9, 14.7, 15 and 86 GHz, we take the weighted average between 4.8 and 5 GHz if both measures are available, we interpolate the remaining values to 2.7 GHz (or extrapolate with $\alpha = -0.1$ if only one frequency measure is left).

We consider the data at 3.9, 14.7, 15 and 86 GHz less reliable for the following reasons: the 3.9 GHz measure may be significantly affected by the ellipticity of the antenna pattern; at 14.7 and 15 GHz the observing resolution is much higher than the typical reference catalogs resolution; at 86 GHz, in addition to the higher resolution, dust emission may contribute largely to the observed flux. Moreover, we prefer to interpolate between 1.4 and 5 GHz rather than extrapolate to 2.7 GHz directly from only one of these two frequencies because we have no information on the frequency location of the free-free knee.

In cases when multiple observations are available at the same frequency, a weighted mean flux density is computed, using the errors discussed below.

For the majority of the sources in the reference catalogs, flux density errors are quoted and these are used in deriving the flux density and its error in the Synthetic Catalog. In the catalogs where no errors are given, an estimate of the error is made by comparing the flux S_* from a catalog without errors with the flux S from a catalog (or some catalogs) giving errors. In particular, we compute the relative (%) dispersion, $\sigma = 100(S_* - S)/S$, and try to fit the resulting distribution in the $S_* - \sigma$ plane with a constant, $\sigma = a$, a linear, $\sigma = a + bS_*$, and a quadratic, $\sigma = a + bS_* + cS_*^2$, dependence of σ on S_*. In these equations the fluxes are in Jy. Before fitting the $\sigma(S_*)$ distribution, we remove the relatively small number of points with a dispersion $\simeq$130%. Although we have considered also fits with a constant, linear, and quadratic dependence of $\log\sigma$ on $\log S_*$, we prefer to use the distributions recovered from the fit carried out with linear variables, since they give, as expected, typical values of $\sigma(S_*)$ larger than those obtained in the case of logarithmic variables and so giving more conservative error estimates. Figure 1 shows the results of the procedure we have described.

An example of the estimates of errors is given by the early Parkes 2.7 GHz catalogs. We compare the list of Parkes sources to the reference catalogs at the same frequency – 2.7 GHz – (namely, Altenhoff et al. 1970; Fürst et al. 1987; Reich et al. 1986; Wendker 1970), in order to retrieve the subset of Parkes sources whose flux has been quoted with an estimated error. In particular, the comparison retrieves 105 sources in common with the Altenhoff et al. (1970) catalog. The scatter σ in the flux density differences, quite well fitted by the law $\sigma \simeq 33.5{-}0.1 \times S$, is comparable to the errors of 10–30% of the Altenhoff et al. catalog alone.

Similar comparisons have been carried out for the Mezger & Henderson (1967) data and for Wink et al. (1983) data. However, as for the Mezger & Henderson data, the comparison with other single catalogs does not provide a significant statistical subset of sources. Therefore, we estimate the error by considering simultaneously the sources from the Mezger & Henderson catalog and from all the other catalogs at 5 GHz (which leads to consider altogether 38 common sources). For the Wink et al. (1983) catalog, we derive an error estimate from the comparison with the Wink et al. (1982) catalog for which we have 21 common sources.

After having estimated the errors on the flux density measures for all catalogs, we compute the errors on the flux densities of the Synthetic Catalog at 2.7 GHz. When an extrapolation with a spectral index $\alpha = -0.1$ from a measure at a single frequency different from 2.7 GHz is applied, we use the standard error propagation rules. No error on α is included in the error propagation, for simplicity.

Table 3 summarizes the errors quoted in the original catalogs and those estimated in this work.

3.2. Angular diameter

We discuss here the assignment of an angular diameter with its associated error for every source in the Synthetic Catalog. The published diameter data are not as comprehensive as the flux density data described in Sect. 3.1; nevertheless we will assign a value of the diameter and an error for each source. For 42% of the sources (derived from the Parkes catalogs and those of Mezger & Henderson 1967; Wendker 1970; Wink et al. 1982; Wink et al. 1983; Berlin et al. 1985) there are no listed diameter errors. For 14% of the sources no diameter is given; for these we derive an indicative diameter.

We assign a diameter for sources in the Synthetic Catalog as follows:

1. when 2.7 GHz diameters are given, we use these values (possibly their weighted average);
2. if there is at least one diameter measure at 5 GHz or at 4.8 GHz, we neglect possible measurements at other frequencies and use this value or, alternatively, the weighted

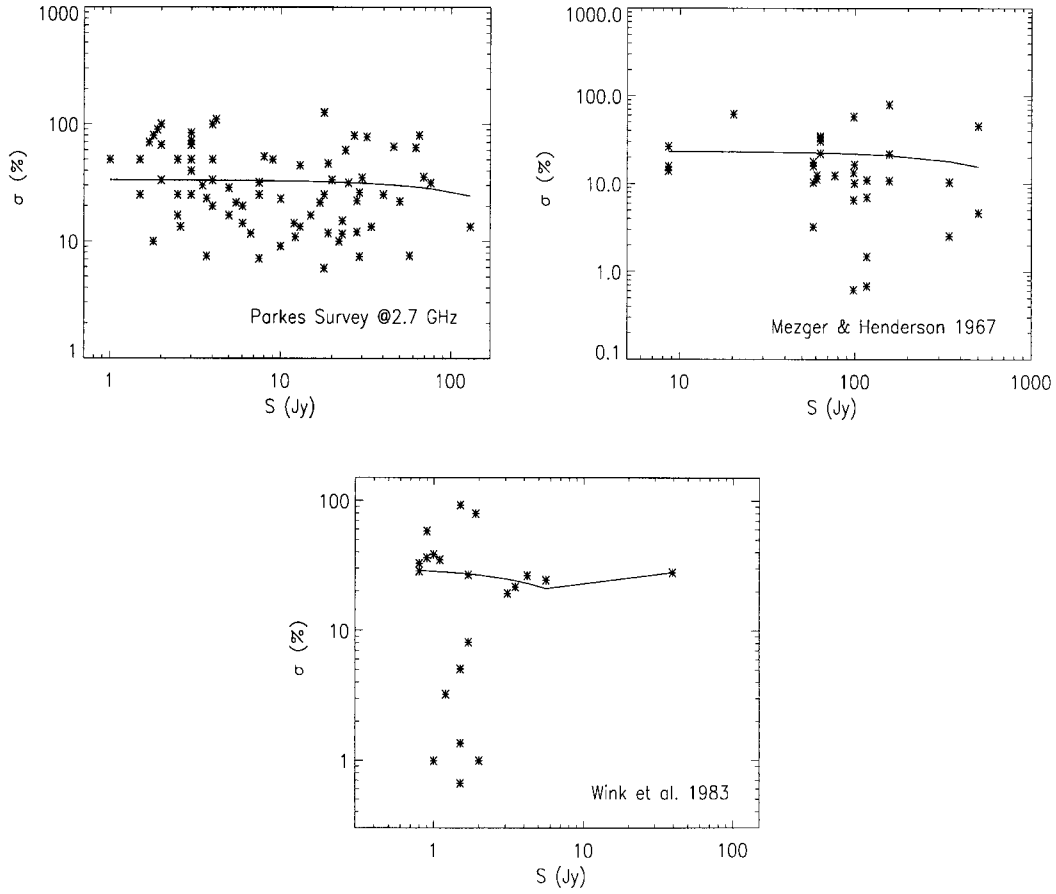

Fig. 1. Results of the flux error estimate for: earlier Parkes survey at 2.7 GHz (top left); Mezger & Henderson (1967) (top right); Wink et al. (1983) (bottom center). Plotted points in each panel correspond to the $\sigma(S_*)$ distribution (where σ is defined as $100(S_* - S)/S$). Overlaid – solid line – is the best fit function. See Sect. 3.1 for more details on the quantities.

average of the diameter measures at 4.8 and 5 GHz when available, using the errors discussed below;

3. if diameter data are given only at frequencies other than ~4.8–5 GHz, we use the weighted average of the available frequencies, after previous exclusion of the measures at $\nu \sim$ 14.7 GHz, using the errors discussed below;
4. if no diameter data is given at frequencies lower than ~14.7 GHz, we use the available measure at 14.7 GHz or at 15 GHz or, alternatively, their weighted average when both values are provided using the errors discussed below (we remember that no diameter data are available at 86 GHz).

Values at 14.7 and 15 GHz are preferably excluded because of the much higher resolution at these frequencies than the typical reference catalog resolution. In each case, when multiple observations are available at the same frequency, a weighted mean is computed, using the errors discussed below.

Finally, we consider the assignment of a diameter to the 14% of HII regions in the Synthetic Catalog which have no quoted diameter in the reference catalogs. It is possible to derive a first-order indicative diameter by noting that the flux density and the diameter of HII regions are weakly correlated, as shown in Fig. 2 which includes all the sources at 2.7 GHz with measured diameters. The best fit to the data gives as

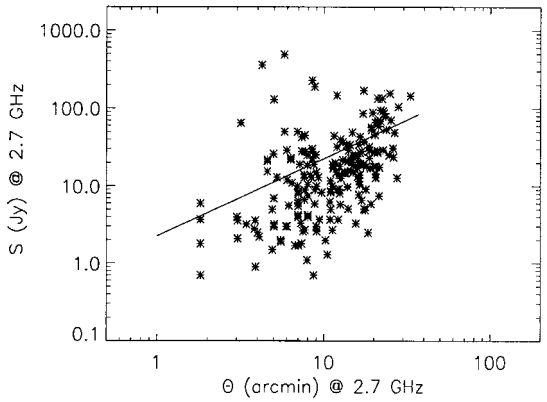

Fig. 2. Correlation between flux densities at 2.7 GHz and angular diameters observed at the same frequency. The solid line represents the best-fit for the plotted distribution.

indicative diameter $\theta = 2.25 \times S$ with a typical error of a factor of 2–3. Each source with an indicative diameter is annotated in the Synthetic Catalog; such diameter data clearly should not be used in astrophysical analysis of the catalog.

Following the same strategy as in Sect. 3.1, where a catalog has no quoted diameter errors we estimate an overall error for that catalog by comparing the observed diameters of that

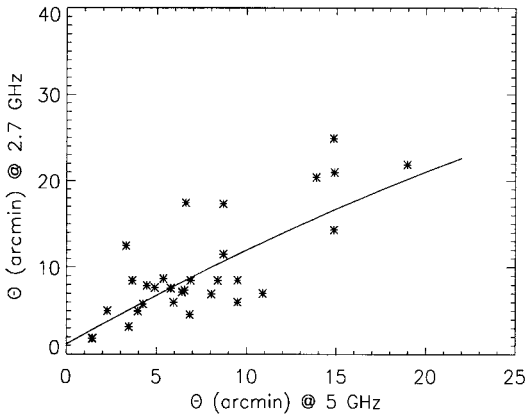

Fig. 3. Diameter measures at 2.7 GHz (y-axis) versus diameter measures and at 5 GHz (x-axis). It is evident the good agreement between the two datasets. The best fit function is: $\Theta_{2.7\ \mathrm{GHz}} = 1.17 + 1.17 \times \Theta_{5\ \mathrm{GHz}}$. Data are from: earlier Parkes survey (2.7 GHz data); Altenhoff et al. (1970)[a], Mezger & Henderson (1967), Reifenstein et al. (1970) (5 GHz data).

catalog with another catalog having an adequate number of sources in common. However, with respect to the flux density case, we can now relax the strict requirement of comparing only different datasets at the same frequency. As shown in Fig. 3, there is no significant frequency dependence in the measured diameters at 2.7 GHz (the Parkes survey) and at 5 GHz (Altenhoff et al. 1970; Mezger & Henderson 1967; Reifenstein et al. 1970). On the other hand, provided that an adequate number of sources in common is retrieved, we prefer to consider in the comparison surveys at the same frequency and with similar angular resolution. Therefore, let Θ_* (Θ) be the source diameter measure in the catalog without quoted errors (with quoted errors). We compute the relative (%) dispersion σ of the diameter measures, $\sigma = 100(\Theta_* - \Theta)/\Theta$, and try to fit the resulting distribution in the $\Theta_* - \sigma$ plane again with a constant, linear, and quadratic, dependence of σ on Θ_* (or of $\log\sigma$ on $\log\Theta_*$; in this case the fit error estimates are again less conservative) and after removing the points with a dispersion $\simeq$130%. In these equations the angular diameters are in arcmin.

Figure 4 shows the results of the error estimates. In particular, we consider the comparison between the following datasets (the first one is that for which we are estimating the errors): Altenhoff et al. (1970)[a] vs. Reifenstein et al. (1970) (48 common sources); Altenhoff et al. (1970)[b] vs. Kuchar & Clark (1997) (63 common sources); Caswell & Haynes (1987) vs. Wilson et al. (1970) (79 common sources); early Parkes 2.7 GHz Survey vs. Reifenstein et al. (1970) (31 common sources); Felli & Churchwell (1972) vs. Kuchar & Clark (1997) (21 common sources); Wendker (1970) vs. Reifenstein et al. (1970) (8 common sources); Wink et al. (1983) vs. Downes (1980) (59 common sources); Wink et al. (1982) vs. Altenhoff et al. (1979) (53 common sources).

As for the Altenhoff et al. (1970) catalog, the data have been split because the diameters have been measured in two different ways: they have been either taken from a survey of Galactic sources made at 5 GHz with the 140-ft antenna – beamwidth 6′ (W. J. Altenhoff, P. G. Mezger and J. Schraml, private communication) – or they have been measured directly from contour maps. We will annotate the set of sources for which the size was measured in the 5 GHz survey Altenhoff et al. (1970)[a] and the remaining sources Altenhoff et al. (1970)[b]. For the Berlin et al. (1985) catalog, since none of the comparisons with other catalogs retrieves a significant number of common sources, we derive the error from the mean of the dispersions σ given by each comparison. Table 3 summarizes the estimated and quoted errors used in calculating the diameters in the Synthetic Catalog.

3.3. Content of the Synthetic Catalog

The Synthetic Catalog summarizes the known radio frequency information on 1442 Galactic HII regions. It contains the position, flux density, diameter data for each HII region, supplemented by velocity data where available. To those HII region with no published diameter data, an indicative diameter is given (marked by $**$) on the basis of the flux-size correlation in Fig. 2. For sake of clarity, the first ten lines of the Synthetic Catalog are reported in Table 2. The line velocity value that we quote in Col. 9 is the weighted average of the available data (see Sect. 2.4 for details). Although the original measures can be, for the same source, at different frequencies, the weighted average of these data is a meaningful quantity and provides a useful first-sight kinematic indication. Since the line velocity is an effect of the Galactic rotation motion, it does not strongly depend on the frequency of observation.

4. Statistical properties of the Synthetic Catalog

The Synthetic Catalog combines the observational data from 24 catalogs with various flux density limits and different angular resolutions. The Kuchar & Clark (1997) catalog, for example, reaches to a sensitivity of 30 mJy but is not sensitive to sources with diameters greater than ∼10′ due to its beam-switching strategy.

Other surveys (e.g. Altenhoff et al. 1970) are sensitive to a wide range of angular scales but include only sources stronger than 1 Jy. We now consider the properties of the sources listed in the Synthetic Catalog in the light of these selection criteria.

4.1. Completeness and flux density limit

A useful way of investigating the completeness of a catalog is to plot the integral count $N(>S)$ as a function of flux density S. Figure 5 shows the integral count for the 1442 sources included in the Synthetic Catalog and for the five contributing catalogs containing more than 200 HII regions. It is evident that the Synthetic Catalog is losing sources fainter than ∼1 Jy. The data in the Synthetic Catalog for $S < 1$ Jy are mainly contributed by the Kuchar & Clark (1997) catalog. Some 50% of the sources at 1 Jy are contributed by this catalog, with a higher fraction at lower flux densities.

The absence of sources at lower flux densities is largely the consequence of source confusion along the Galactic plane. For example, in the region $|l| < 60°$ there are 1200 Synthetic Catalog sources within the Galactic plane ($|b| < 2°$); in a 10′ beam (or a 10′ diameter source) there is one HII region per 15 beam area which represents a significant confusion level.

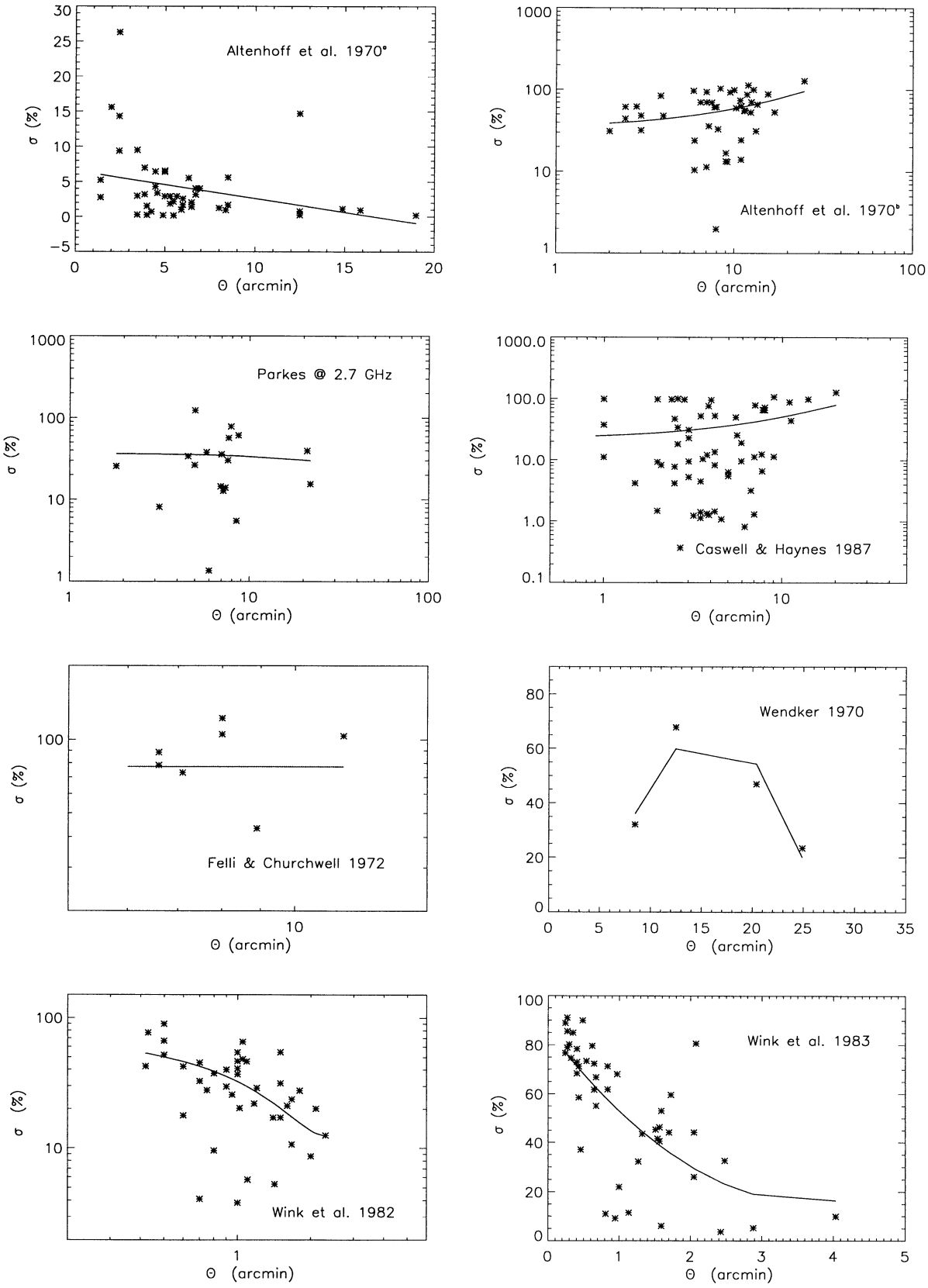

Fig. 4. Results of the diameter error estimate for: Altenhoff et al. (1970)^a (top left); Altenhoff et al. (1970)^b (top right); earlier Parkes survey at 2.7 GHz (left, second row); Caswell & Haynes (1987) (right, second row); Felli & Churchwell (1972) (left, third row); Wendker (1970) (right, third row); Wink et al. (1982) (bottom left); Wink et al. (1983) (bottom left). Plotted points in each panel correspond to the $\sigma(\Theta_*)$ distribution (where σ is defined as $100(\Theta_* - \Theta)/\Theta$). Overlaid – solid line – is the best fit function. See Sect. 3.2 for more details on the quantities.

Table 2. A selection of sources from the Synthetic Catalog is shown. The arrangement of column is as follows:
- Column 1: source-numbering (records from 1 to 1442)
- Columns 2–3: galactic coordinates, l and b
- Columns 4–5: celestial coordinates (epoch 2000)
- Columns 6–7: derived 2.7 GHz flux density and 1–σ error (Jy)
- Columns 8–9: derived angular diameter and 1–σ error (arcmin)
- Columns 10–11: velocity relative to the LSR and 1–σ error (km s^{-1})
- Column 12: notes on individual sources (see Sect. 2.4 and Appendix 1 for details).

N	l	b	RA	DEC	S	σ_S	θ	σ_θ	$V_{\rm LSR}$	$\sigma_{V_{\rm LSR}}$	Notes
1	0.1	0.0	17 45 51.3	−28 51 08	230.0	24.1	5.9	0.5	−27.4	4.0	W24
2	0.2	−0.1	17 46 29.0	−28 49 07	209.4	10.5	10.7	0.5	24.5	3.5	
3	0.2	−0.0	17 46 05.6	−28 46 00	177.6	38.1	9.2	0.5	−12.7	3.5	W24
4	0.3	−0.5	17 48 17.0	−28 56 25	2.5	0.7	2.7	1.7	20.0	4.9	C, S
5	0.4	−0.8	17 49 41.7	−29 00 33	8.0	2.6	7.0	2.3	20.0	4.9	C, S
6	0.4	−0.5	17 48 31.1	−28 51 17	4.1	1.0	3.9	1.8	24.0	4.9	C, S
7	0.5	−0.7	17 49 32.2	−28 52 19	2.9	0.9	2.3	1.4	17.5	4.9	C
8	0.5	−0.1	17 47 11.6	−28 33 44	28.3	4.0	3.3	1.4	45.8	5.0	S, X
9	0.5	0.0	17 46 48.2	−28 30 37	40.3	8.6	4.8	0.3	47.1	2.0	
10	0.6	−0.9	17 50 33.3	−28 53 19	2.5	0.8	2.4	1.3	15.0	4.9	S, S21, RCW142

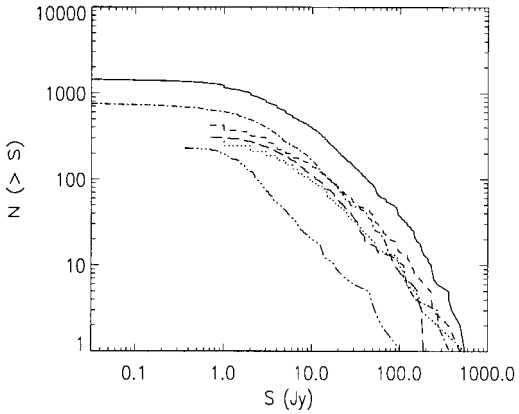

Fig. 5. Cumulative counts, $N(>S)$, for the Synthetic Catalog (solid line) and 5 contributing catalogs: Kuchar & Clark (1997) (dash-dot line), early Parkes 2.7 GHz catalogs (dashed line), Caswell & Haynes (1987) (long-dash line), Altenhoff et al. (1970) (dotted line), Altenhoff et al. (1979) (three dots-dashes).

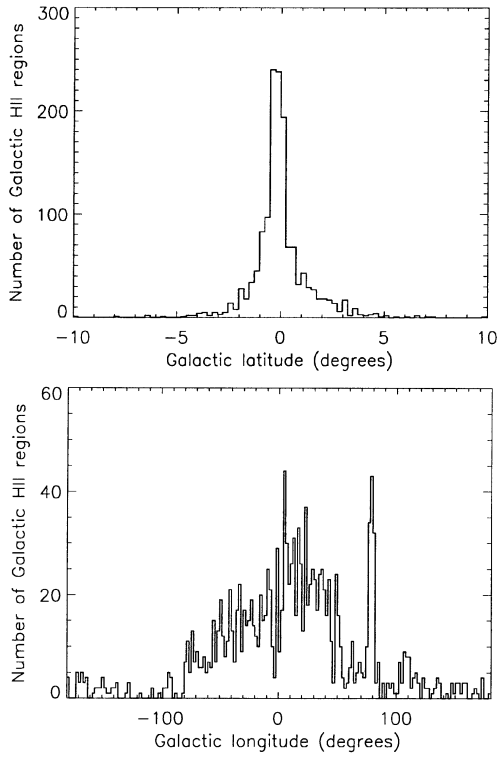

Fig. 6. Top panel: Galactic latitude distribution of the HII regions of the Synthetic catalog. The mean Galactic latitude is is $b = 0.05°$. Bottom panel: Galactic longitude distribution.

It is clearly difficult to resolve into individual sources the structure seen in the central regions of the Galaxy. The majority, ∼150, of the weaker (< 1 Jy) sources catalogued by Kuchar & Clark are in the less complex regions of the Galaxy such as the anticentre region (quadrants 2 and 3) – 73 sources – and Galactic latitudes greater than 1° ($|b| > 1°$) in quadrants 1 and 4 – 19 sources –.

4.2. Spatial distribution

The Galactic latitude and longitude distribution of the HII regions in the Synthetic Catalog are shown in Fig. 6. A striking feature is the narrow distribution in Galactic latitude where the full width at half power is 0.95° when averaged over all longitudes; the mean Galactic latitude is $b = 0.05°$. This narrow distribution will reflect the distribution of the O and B stars responsible for the ionization.

The main concentration in longitude is at $|l| < 60°$ where the line of sight cuts the spiral arms internal to the local arm in which the Sun lies. There are also discernable peaks at $l \sim \pm 80°$ associated with the local arm; the peak at $l \sim 80°$ is the Cygnus X region where Wendker (1970) identified 77 HII regions in his survey. There is a clear deficit of sources in the anticentre region of the Galaxy (l = 90°–270°). Although there is a less complete coverage in this sector of the Galactic plane as indicated in Table 1, the large deficit of sources is real.

The optical study of the distribution of HII regions in the outer Galaxy by Fich & Blitz (1984) indicate that they are limited to $R < 20$ Kpc.

5. Applications of the Synthetic Catalog

An extensive data base of radio observations of HII regions has been distilled into the Synthetic Catalog of 1442 objects at a frequency of 2.7 GHz. We consider some uses of this catalog and the associated Master Catalog for studies of individual HII regions over a range of frequencies and for CMB studies.

5.1. Detectability of HII regions

The sensitivity of a particular instrument in Kelvin to an HII region of a given flux density expressed in Jansky depends upon the observing frequency ν, the beamwidth (*FWHM*), the sensitivity per second of integration and the observing time t (the rms noise decreases with observing time t as $t^{-\frac{1}{2}}$). The rms noise in Jansky per second of integration, $\mathrm{rms}_{1s,f}$, is related to the rms antenna temperature in Kelvin per second of integration, $\mathrm{rms}_{1s,a}$, by:

$$(\mathrm{rms}_{1s,f}/\mathrm{Jy}) = 2.95 \times 10^{-3} (FWHM/\mathrm{arcmin})^2 \cdot (\nu/\mathrm{GHz})^2 (\mathrm{rms}_{1s,a}/\mathrm{K}) \quad (1)$$

and the same relation holds between the source signal expressed in terms of flux density or of antenna temperature. Here the source is assumed to be point-like and observed at the centre of a Gaussian, symmetric beam. Eq. (1) can be then used to determine the S/N for a point source of a given flux density. In cases when a source with a diameter comparable or bigger than the *FWHM* of the observing beam is considered, a correcting factor to Eq. (1) is required to compute the S/N. In particular, the S/N is ∼40 to 90% the value computed with Eq. (1) when a source with a diameter ∼2–3 times the beamwidth or ∼1/2–1/3 the beamwidth, respectively, is considered. The S/N represents an easy way to compare the signal produced by Galactic HII regions with the sensitivity of a typical CMB anisotropy experiment. Therefore, we apply the above treatment to the high resolution satellite experiment Planck by ESA[1], scheduled for launch in 2007. Planck will observe the entire sky with a sensitivity at the end of the mission of about 10 μK per resolution element. The beamwidths vary between ∼33.6′ and 5′ from 30 to 857 GHz respectively. For numerical estimates, we consider here the channels at 30 and 100 GHz which have a nominal *FWHM* of ∼33.6′ and 10′. For comparison, we make the same calculation for *COBE*-DMR for which, at 31.5 and 90 GHz the rms temperature was 150 and 100 μK and the beamwidth was 7° (Boggess et al. 1992).

The S/N for all the HII regions in the Synthetic Catalog have been calculated as discussed above; the flux densities were estimated at each frequency from 2.7 GHz values assuming a flux density proportional to $\nu^{-0.1}$. Figure 7 shows the number of sources per bin of S/N (the distribution function) and number of sources greater than a certain S/N (cumulative distribution function) for both Planck and *COBE*-DMR at ∼30 and ∼100 GHz.

From Fig. 7 it is clear that the vast majority of sources in the Synthetic Catalog produces a signal which highly exceeds the detection threshold of the instrument. Therefore, not only all the Synthetic Catalog HII regions will be detected but also 80% of these sources will have a $S/N > 100$ (while the weakest sources, with $S \sim 10$ mJy, will be seen with a $S/N \sim 3$). As a consequence, Planck high sensitivity and high resolution should allow to significantly entend the existing HII regions data base. It is important to emphasize that none of the individual HII regions would have been seen by *COBE*-DMR whose flux sensitivity according to Eq. (1) is 6×10^3 less than Planck at 30 GHz and 4×10^4 less at 100 GHz.

5.2. Radio/millimeter studies of HII regions

The ionizing radiation from the central O/B stars produces the HII region which emits through the free-free mechanism from radio to submillimetric wavelenghts; the surrounding dust is also heated by radiation originally derived from the central stars and as a consequence radiates at submillimeter and IR wavelenghts. The flux density of the radiation from these two components was found to be equal in the wavelenght range 1–3 mm (100 to 300 GHz) by Kurtz et al. (1994) for a selection of compact HII regions. However, many interesting questions remain to be resolved in the physical relationship between the HII region and the radiation-heated dust cloud in which it is embedded. The Synthetic Catalog provides a rich source of HII regions for further study. Figure 7 shows that many hundreds of HII regions will be detectable at high sensitivity and with adequate resolution over the frequency range 30 to 857 GHz by Planck. Thus, this may represent a good chance for a comparative study of the far-IR and radio continuum morphology of Galactic HII regions.

Moreover, source identification in IR experiments such as DENIS (Epchetein et al. 1994) and 2MASS (Kleinmann 1992) can benefit from the crosscheck with the Synthetic Catalog. In fact, for these kind of experiments a major problem is the association of an observed source with a bright IR Galactic object like an HII region or an ultracompact HII region rather than with an external Galaxy.

5.3. Use of the Synthetic Catalog in CMB studies

We will consider in this subsection several applications of the Synthetic Catalog in CMB studies. The first use we discuss is the production of maps of the integrated free-free emission as seen with the angular resolution of an instrument such as Planck at each observing frequency. Free-free emission dominates the Galactic plane signal at least over the range 30 to 100 GHz. Figure 8 shows the Galactic plane emission resulting from HII regions as seen by Planck at 30 GHz where the beamwidth is 33.6′.

To make the map in Fig. 8, we have implemented a code which simulates the contribution of each source in the Synthetic Catalog at a given angular resolution by assuming

[1] http://planck.esa.nl

Table 3. Summary of relative (%) errors on quoted fluxes and diameters in the corresponding sub-catalogs. Errors marked by $*$ have been estimated by the authors of the present paper. Errors marked by $**$ correspond to the indicative diameters estimated by means of the flux-size correlation in Fig. 2. Further details in Sects. 3.1 and 3.2.

Reference	% flux error	% size error
Altenhoff et al. (1970)[a]	10/30	6.5–0.4×Θ (∗)
Altenhoff et al. (1970)[b]	10/30	33.9+2.5×Θ (∗)
Altenhoff et al. (1979)	5	10
Beard (1966)	33.5–0.1×S (∗)	300 (∗∗)
Beard & Kerr (1969)	33.5–0.1×S (∗)	37–0.3×Θ (∗)
Beard et al. (1969)	33.5–0.1×S (∗)	37–0.3×Θ (∗)
Berlin et al. (1985)	10	72.5 (∗)
Caswell & Haynes (1987)	10	22.1+2.8×Θ (∗)
Day et al. (1969)	33.5–0.1×S (∗)	300 (∗∗)
Day et al. (1970)	33.5–0.1×S (∗)	300 (∗∗)
Downes et al. (1980)	5	10
Felli & Churchwell (1972)	15/35	77.4 (∗)
Fürst et al. (1987)	10	300 (∗∗)
Goss & Day (1970)	33.5–0.1×S (∗)	37–0.3×Θ (∗)
Kuchar & Clark (1997)	10/20	16/25
Mezger & Henderson (1967)	23.3(∗)	20/50
Reich et al. (1986)	10	300 (∗∗)
Reifenstein et al. (1970)	15	3
Thomas & Day (1969a)	33.5–0.1×S (∗)	300 (∗∗)
Thomas & Day (1969b)	33.5–0.1×S (∗)	300 (∗∗)
Wendker (1970)	6	–73.6+17.6×Θ–0.5×Θ^2
Wilson et al. (1970)	15	5
Wink et al. (1982)	5/15	73.5–52.1×Θ+11.1×Θ^2 (∗)
Wink et al. (1983)	30.3–1.9×S +0.1× S^2 (∗)	85.8–38.1×Θ+5.2×Θ^2 (∗)

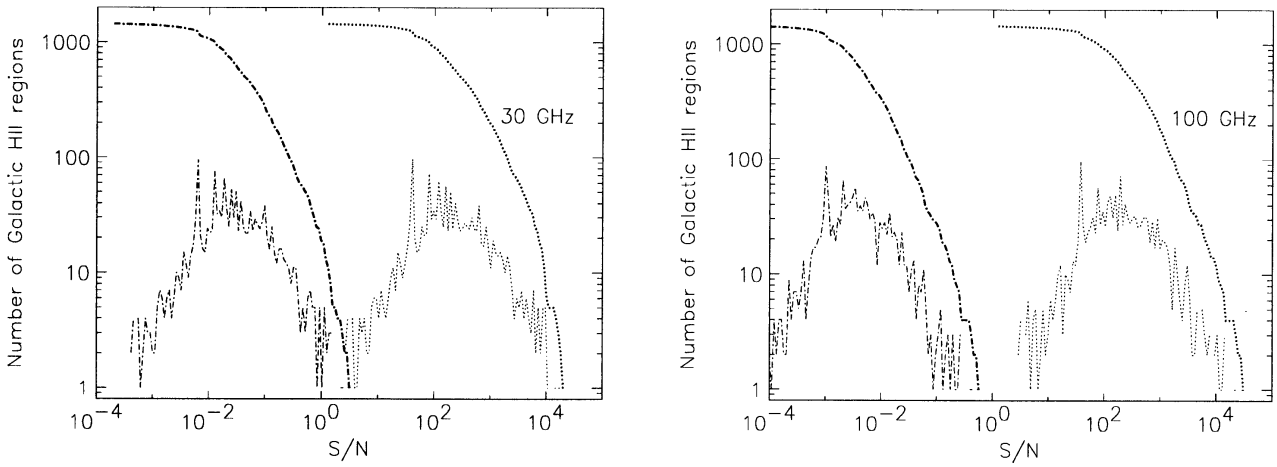

Fig. 7. Distribution functions (bottom curves) and cumulative distribution functions (upper curves) at 30 and 100 GHz for Planck (dotted lines) and *COBE*-DMR (dash-dot lines). The *COBE*-DMR angular resolution is 7° at both frequencies.

a symmetric Gaussian profile for the source brightness distribution and numerically convolves, in real space, the relevant part of the map – obtained after considering the contribution from all the sources in the catalog – with another symmetric Gaussian profile having the instrument *FWHM*. The final map is generated in HEALPix (Hierarchical Equal Area and IsoLatitude Pixelization of the Sphere, by Górski et al. 1998). Figure 9 shows the strong Galactic centre and Cygnus X regions. Antenna temperature as high as ∼50 mK are seen.

Moreover, HII regions, as delineated in Fig. 8, can in principle represent a significant contribution – comparable to that produced by synchrotron and dust emission – to one of the most critical spurious effects in CMB surveys, the so-called straylight contamination through their integrated signal in the sidelobes (Burigana et al. 2001) which needs to be properly evaluated. The optical design of Planck and similar mapping instruments must be optimized to minimize this effect. In any case, the residual straylight should be taken into account in the data analysis.

HII regions also have a part to play in CMB imaging experiments as suitable calibrators and as probes of the pointing and beamshape. HII regions are non-variable and have quite

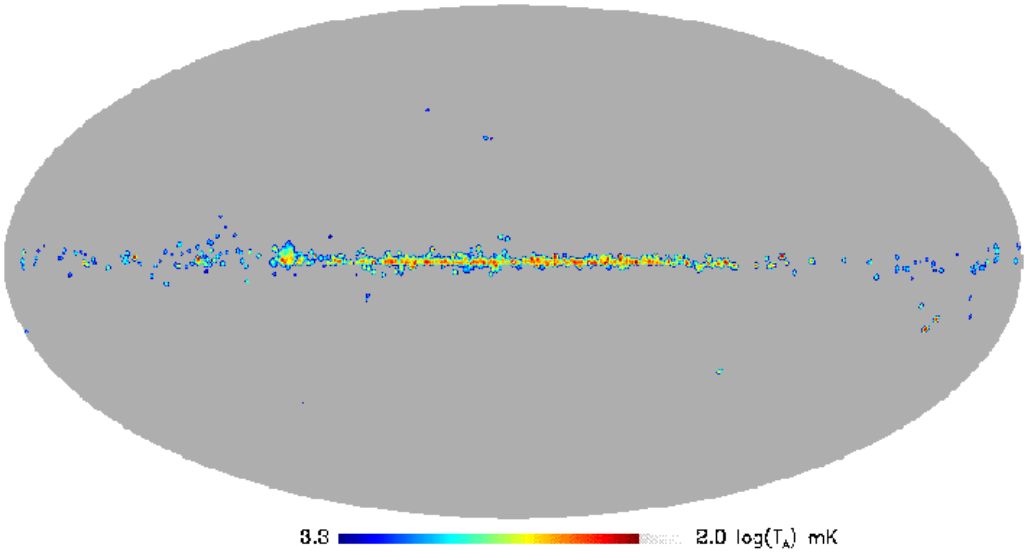

Fig. 8. Simulated full sky map of the antenna temperature signal at 30 GHz produced by the Synthetic Catalog HII regions for an instrument with a *FWHM* of 33.6′. The map is displayed in all-sky mollweide projection. The color bar shows the minimun and maximum of the pixels in the map with a positive signal. The signal looks particularly bright with peaks of tens of mK. See also the text.

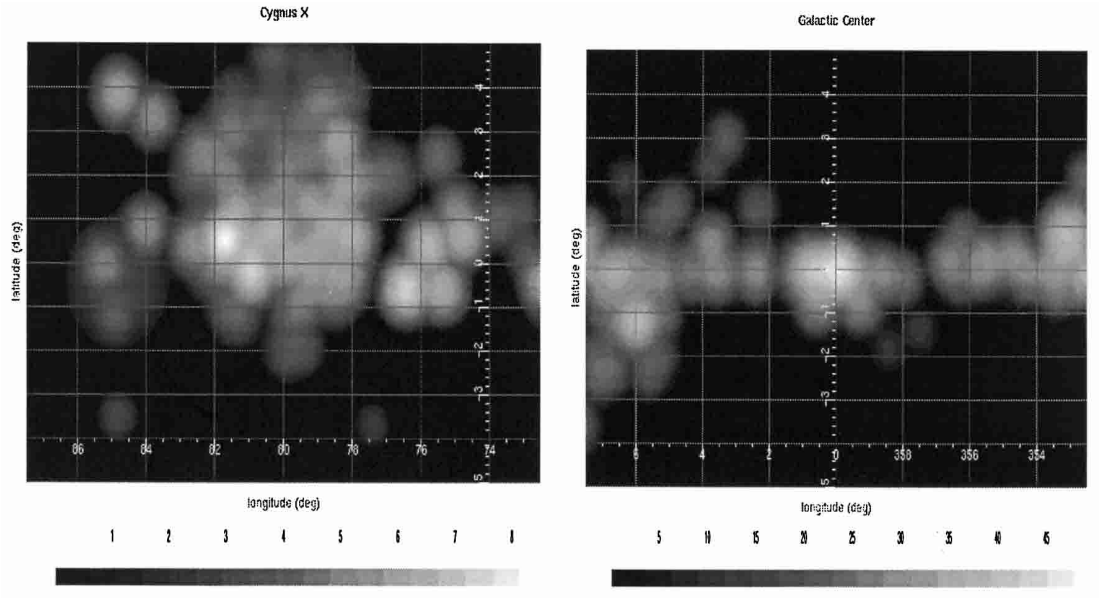

Fig. 9. Simulated maps of the Cygnus X region (left panel) and of the Galactic Center region (right panel) at 30 GHz with a *FWHM* resolution of 33.6′. The units of the color bar are mK. Minimum and maximum refer to positive pixel signal values.

a well-known spectrum which makes them valuable calibrators along with planets and the CMB dipole (Bersanelli et al. 1997). In addition, for space missions, they provide auxiliary data for inflight beam reconstruction and pointing by complementing the information from planet transits (Burigana et al. 2002) and from the interplay between amplitudes and phases of CMB signal with the instrumental noise (Chiang et al. 2002). In particular, the Chiang et al. method, although not requiring the use of bright sources, allows the reconstruction of the beam ellipticity only in the beam central regions while the Burigana et al. technique allows the complete reconstruction of the beam shape down to a level of −25 dB but makes use of non-variable, bright, compact sources. However, despite being originally conceived for planets, the Burigana et al. method can be easily extended to other classes of sources which also enable to increase the number of transits over the space mission lifetime. The Synthetic Catalog contains 36 HII regions which have a flux density ≥30 Jy at 30 GHz and a diameter ≤ than 5′. Accurate flux densities ad positions can be determined from ground-based aperture synthetis observations.

Finally, we point out that the angular extension of a typical Galactic HII region represents an intermediate case between point sources and diffuse foregrounds for which component separation tools have been specifically designed (see, e.g., Maino et al. 2001, and references therein). The fluctuations produced by such extended sources and the capability of

existing component separation methods to handle with them will have to be furtherly investigated in the next years.

6. Conclusions

We have collected radio data of Galactic HII regions from 24 published works and built a self-consistent database of 1442 sources. This work has resulted in the construction of what we have called Master Catalog which consists in 11 different sub-catalogs storing the original information from the source references. In particular, the sub-catalogs list flux densities and diameters as well as radio line velocities, line widths and line temperatures; errors are given on these quantities.

From this large data set observed at a range of frequencies and beamwidths, we have produced a readibily accessible Synthetic Catalog giving the flux density, diameter and velocity (where available) at 2.7 GHz, the frequency where most data are given. Errors on these observed parameters are derived using the procedures discussed in Sect. 3.

It should be emphasized that the Catalog is a compilation of published radio data on HII regions; it is not a complete survey down to the faintest flux density level listed. We argue in Sect. 4 that it is probably complete to a flux density of 1 Jy. Nevertheless, the Catalog provides an up to date finding list for the brightest HII regions available for further study at microwave and submillimeter wavelenghts. The Synthetic Catalog is also particularly relevant to future high sensitivity CMB mapping projects such as Planck. We have shown in Sect. 5 that the HII region Galactic distribution can contribute to the straylight radiation, while individual compact bright HII regions have a role as calibrators and as pointing and beamshape indicators.

The Master Catalog and the Synthetic Catalog are only available via anonymous ftp to `cdsarc.u-strasbg.fr (130.79.128.5)` or via `http://cdsweb.u-strasbg.fr/cgi-bin/qcat?J/A+A/397/213`

Color figures can be obtained via e-mail request to `paladini@sissa.it`.

Acknowledgements. We wish to thank C. Witebsky for providing us with the *COBE*-HII compilation and T. A. Kuchar and F. O. Clark for making their radio and IRAS data available prior to publication. The authors made use of the database CATS (Verkhodanov et al. 1997) of the Special Astrophysical Observatory. We are also grateful to G. De Zotti and H. J. Wendker for useful discussions and suggestions. We thank L. Cambrecy for valuable comments to our work. R. Paladini acknowledges financial support from a NATO International Exchange Scientific Programme grant and from a Marie Curie Training Site fellowship. We gratefully acknowledge K. M. Górski and all the people involved in the realization of the tools of HEALPix pixelisation.

Appendix I: The Master Catalog

The Master Catalog contains the original data taken from the source references of Table 1. Due to the extensive amount of information, we have divided for convenience the Master Catalog into 11 sub-catalogs. We give hereafter the description of the structure of each of these compilations while, for a general overview about the content of the sub-catalogs, we refer the reader to Sect. 2.5.

As mentioned in the main text (Sect. 2.5), each sub-catalog (except for Sub-catalog 1) has 37 columns and 1442 entries corresponding to the total number of sources. The columns are in order of increasing frequency of observation and, at each frequency, the columns are in alphabetical order of the references in Table 1. In all sub-catalogs, a null entry corresponds to no information available from the source reference.

Sub-catalog 1 lists only source coordinates, notes about the environment and radio/optical couterparts. For its content specificy, it presents a peculiar structure with respect to the other sub-catalogs. In detail:
- Column 1: source-numbering (records from 1 to 1442)
- Columns 2–3: Galactic coordinates, l and b
- Columns 4–6: celestial coordinates: RA – J2000
- Columns 7–9: celestial coordinate: DEC – J2000
- Column 10: general remarks - C = complex field, S = strong source nearby, X = strong source nearby (>10 Jy), radio or optical counterpart. This flags follow the definitions given by Kuchar & Clark (1997) according to which a source is in a complex field when there are two or more sources within either $2\times\Theta_{\rm obs}$ (i.e, four source radii) or $2\times\Theta_{\rm beam}$, whatever is larger[2], or with a strong and/or much stronger source nearby.

As for the counterpart in other wavebands, for the case of the radio identifications: Ke refers to Kesteven (1968); NRAO to Pauliny-Toth (1966); W to Westerhout (1958); 3C to Third Cambridge Catalog (Bennett 1962) and 4C to Fourth Cambridge Catalog (Gower et al. 1967; Pilkington et al. 1965).

For the optical identifications, the Mársalková Catalog 1974 has been consulted. In this case: BBW refers to Bok-Bester-Wade (1955); DWB to Dickel-Wendker-Bieritz (1969); Ge (a) to Georgelin-Georgelin (1970a); Ge (b) to Georgelin-Georgelin (1970b); Ge (c) to Georgelin-Georgelin (1970c); G to Gum (1955); H to Hoffleit (1953); RCW to Rodgers-Campbell-Whiteoak (1960); S to Sharpless (1959). Moreover, M stands for Messier Catalog; NGC for Dreyers'New General Catalog and IC for the Index Catalog.

Sub-catalog 2 to sub-catalog 11 have the following structure:
- Column 1: source-numbering (records from 1 to 1442);
- Columns 2–3: Galactic coordinates, l and b;
- Columns 4–6: celestial coordinates: RA – J2000;
- Columns 7–9: celestial coordinate: DEC – J2000;
- Columns 10–11: 1.4 GHz – Altenhoff et al. (1970), Felli & Churchwell (1972);
- Columns 12–23: 2.7 GHz – Altenhoff et al. (1970), Beard (1966), Beard & Kerr (1969), Beard et al. (1969), Day et al. (1969), Day et al. (1970), Fürst et al. (1987), Goss & Day (1970), Reich et al. (1986), Thomas & Day (1969a), Thomas & Day (1969b), Wendker (1970);
- Column 24: 3.9 GHz – Berlin et al. (1985);
- Columns 25–26: 4.8 GHz – Kuchar & Clark (1997);
- Columns 27–34: 5 GHz – Altenhoff et al. (1970), Altenhoff et al. (1979), Caswell & Haynes (1987), Downes et al. (1980),

[2] In Kuchar & Clark's paper, fluxes and angular sizes are measured directly from the survey images.

Mezger & Henderson (1967), Reifenstein et al. (1970), Wilson et al. (1970), Wink et al. (1982);
- Column 35: 14.7 GHz – Wink et al. (1983);
- Column 36: 15 GHz – Wink et al. (1982);
- Column 37: 86 GHz – Wink et al. (1982).

Note on sub-catalog 2 and sub-catalog 4: these sub-catalogs, including data on flux and angular diameters, always list values corrected for the instrument beam. Their complementary sub-catalogs are sub-catalog 3 and 5 quoting relative (%) errors.

Note on sub-catalog 6 to 11: these sub-catalogs list line velocity data. Observations may refer to frequencies other than those for the continuum data. In particular:
- Columns 25–26: Kuchar & Clark quote continuum data at 4.85 GHz and line data from Reifenstein et al. (1970) and from Wilson et al. (1970) at 5 GHz (H109α) and from Lockman (1989) at 10 GHz (H85α, H87α and H88α);
- Column 28: Altenhoff et al. (1979) quotes continuum data at 5 GHz while line data are taken from Lockman (1989) at 10 GHz (H85α, H87α and H88α);
- Columns 29–33: Caswell & Haynes (1987), Downes et al. (1980), Mezger & Henderson (1967), Reifenstein et al. (1970), Wilson et al. (1970) quote both continuum and line data at 5 GHz (H109α, H110α);
- Columns 34–36–37: Wink et al. (1982) quotes continuum data at 5/15/86 GHz and line data at 8.9/14.7 GHz (H90α and H76α).

References

Altenhoff, W. J., Downes, D., Goad, L., Maxwell, A., & Rinehart, R. 1970, A&AS, 1, 319

Altenhoff, W. J., Downes, D., Pauls, T., & Schraml, J. 1979, A&AS, 35, 23

Beard, M. 1966, Aust. J. Phys., 19, 141

Beard, M., & Kerr, F. J. 1969, Aust. J. Phys., 22, 121

Beard, M., Thomas, B., Mac, A., & Day, G. A. 1969, Aust. J. Phys. Suppl., 11, 27

Becker, R. H., White, R. L., Helfand, D. J., & Zoonematkermani, S. 1994, ApJS, 91, 347

Bennett, A. S. 1962, Mem. R. Astr. Soc., 68, 163

Berlin, A. B., Gol'nev, V. Y., Lipovka, N. M., Nizhel'skij, N. A., & Spangenberg, E. E. 1985, AZh, 62, 229

de Bernardis, P., Ade, P. A. R., Bock, J. J., et al. 2000, Nature, 404, 955

Bersanelli, M., Muciaccia, P. F., Natoli, P., Vittorio, N., & Mandolesi, N. 1997, A&AS, 121, 393

Boggess, N. W., Mather, J. C., Weiss, R., et al. 1992, ApJ, 297, 420

Bok, B. J., Bester, M. J., Wade, C. M. 1955, Daedalus, Harvard Reprint, 416, 1

Burigana, C., Natoli, P., Vittorio, N., Mandolesi, N., & Bersanelli, M. 2002, Exp. Astron., 12/2, 87

Burigana, C., Maino, D., Górski, K. M., et al. 2001, A&A, 373, 345

Caswell, J. L., & Haynes, R. F. 1987, A&A, 171, 261

Chiang, L.-Y., Christensen, P. R., Jorgensen, H. E., et al. 2002, A&A, 392, 369

Condon, J. J., Broderick, J. J., & Seielstad, G. A. 1989, AJ, 97, 1064

Condon, J. J., Griffith, M. R., & Wright, A. E. 1993, AJ, 106, 1095

Day, G. A., Thomas, B., Mac, A., & Goss, W. M. 1969, Aust. J. Phys. Suppl., 11, 11

Day, G. A., Warne, W. G., & Cooke, D. J. 1970, Aust. J. Phys. Suppl., 13, 11

Dickel, H. R., Wendker, H., & Beiritz, J. H. 1969, A&A, 1, 270

Downes, D., Wilson, T. L., Bieging, L., & Wink, J. 1980, A&AS, 40, 379

Duncan, A. R., Stewart, R. T., Haynes, R. F., & Jones, K. L. 1995, MNRAS, 277, 36

Epchtein, N., et al. 1994, Astr. Sp. Sci., 217, 3

Felli, M., & Churchwell, E. 1972, A&AS, 5, 369

Fich, M., & Blitz, L. 1982, ApJS, 49, 183

Fich, M., & Blitz, L. 1984, ApJ, 279, 125

Fürst, E., Handa, T., Reich, W., Reich, P., & Sofue, Y. 1987, A&AS, 69, 403

Fürst, E., Reich, W., Reich, P., & Reif, K. 1990a, A&AS, 85, 691

Fürst, E., Reich, W., Reich, P., & Reif, K. 1990b, A&AS, 85, 805

Georgelin, Y. P., & Georgelin, Y. M. 1970a, A&A, 6, 349

Georgelin, Y. P., & Georgelin, Y. M. 1970b, A&A, 7, 133

Georgelin, Y. P., & Georgelin, Y. M. 1970c, A&AS, 3, 1

Górski, K. M., Hivon, E., & Wandelt, B. D. 1998, Proceedings of the MPA/ESO Conference on Evolution of Large-Scale Structure: from Recombination to Garching, ed. A. J. Banday, R. K. Sheth, & L. Da Costa, 37 [astro-ph/9812350]

Goss, W. M., & Day, G. A. 1970, Aust. J. Phys. Ap. Suppl., 13, 3

Gower, J. F. R., Scott, P. F., & Wills, D. 1967, Mem. R. astr. Soc., 71, 49

Green, D. A. 2000, A Catalog of Galactic Supernova Remnants (2000 August version), Mullard Radio Astronomy Observatory, Cavendish Laboratory (Cambridge, United Kingdom)

Gum, C. S. 1955, Memoirs RAS, 67, 155

Hanany, S., Ade, P., Balbi, A., et al. 2000, ApJ, 545, 5

Hoffleit, D. 1953, Ann. Harv. Coll. Observ., 119, 37

Israel, F. P., & Van der Kruit, P. C. 1974, A&A, 32, 363

Kesteven, M. J. L. 1968, Austr. J. Phys., 21, 369

Kleinmann, S. G. 1992, Robotic Telecopes in the 1990s, ASP Conf. Ser., 203

Kraus, J. D. 1966, Radio Astronomy (McGraw-Hill, New York)

Kuchar, T. A., & Clark, F. O. 1997, ApJ, 488, 224

Kurtz, S., Churchwell, E., & Wood, D. O. S. 1994, ApJS, 91, 659

Leitch, E. M., Pryke, C., Halverson, N. W., et al. 2002, ApJ, 568, 28L

Lockman, F. J. 1989, ApJS, 71, 469

Lockman, F. J., Pisano, D. J., & Howard, G. J. 1996, ApJ, 472, 173

Maino, D., Farusi, A., Baccigalupi, C., et al. 2002, MNRAS, 334, 53

Màrsalkovà, P. 1974, A&SS, 27, 3

Mason, B., CBI collaboration 2001, AAS, 199, 3402S

Mezger, P. G., & Henderson, A. P. 1967, ApJ, 147, 471

Pauliny-Toth, I. I. K., Wade, C. M., & Heeschen, D. S. 1966, ApJS, 13, 65

Pilkington, J. D. H., & Scott, P. F. 1965, Mem. R. Astr. Soc., 69, 183

Reich, W., Fürst, E., Haslam, C. G. T., Steffen, P., & Reif, K. 1984, A&AS, 58, 179

Reich, W., Fürst, E., Reich, P., Sofue, Y., & Handa, T. 1986, A&A, 155, 185

Reich, W., Fürst, E., Reich, P., & Reif, K. 1990, A&AS, 85, 633

Reifenstein, E. C., Wilson, T. L., Burke, B. F., Mezger, P. G., & Altenhoff, W. J. 1970, A&A, 4, 357

Rodgers, A. W., Campbell, C. T., & Whiteoak, J. B. 1960, MNRAS, 121, 103

Rohlfs, K. 1990, Tools of Radio Astronomy (Springer & Verlag, Berlin)

Scott, P. F., VSA collaboration [astro-ph/0205380]

Sharpless, S. 1959, ApJS, 4, 257S

Smoot, G. F., Bennett, C. L., Kogut, A., et al. 1992, ApJ, 396, L1
Tasker, N. J., Condon, J. J., Wright, A. E., et al. 1994, AJ, 107, 2115
Taylor, A. R., Goss, W. M., Coleman, P. H., Van Leeuwen, J., & Wallace, B. J. 1996, ApJS, 107, 329
Thomas, B., & Day, G. 1969a, Aust. J. Phys. Suppl., 11, 3
Thomas, B., & Day, G. 1969b, Aust. J. Phys. Suppl., 11, 19
Verkhodanov, O. V., Trushkin, S. A., Andernach, H., & Chernenkov, V. N. 1997, The CATS database to operate with astrophysical catalogs – Astronomical Data Analysis Software and Systems VI, ed. G. Hunt & H. E. Payne, ASP Conf. Ser., 125, 322
Wendker, H. J. 1970, A&A, 4, 378
Westerhout, G. 1958, B.A.N, 14, 21
Wilson, R. W., & Bolton, J. G. 1960, P.A.S.P., 72, 331
Wilson, T. L., Mezger, P. G., Gardner, F. F., & Milne, D. K. 1970, A&A, 6, 364
Wink, J. E., Altenhoff, W. J., & Mezger, P. G. 1982, A&A, 108, 227
Wink, J. E., Wilson, T. L., & Bieging, J. H. 1983, A&A, 127, 211
Witebsky, C. 1978a, *COBE* NOTE # 5006, Internal Report
Witebsky, C. 1978b, *COBE* NOTE # 5013, Internal Report